

## Photoinduced Effects in UV Laser Melting of Si in UHV

Bogdan Dragnea and Bernard Bourguignon\*

*Laboratoire de Photophysique Moléculaire du CNRS, Bâtiment 210 Université de Paris-Sud, 91405 Orsay Cedex, France*

(Received 23 February 1998; revised manuscript received 20 November 1998)

The dynamics of laser heating and melting of Si in UHV is investigated by transient reflectivity with single pulse sensitivity. It is found that the heating and melting dynamics cannot be accounted for by a model of heat flow using the thermal and optical properties of Si. Experiment and theory can be reconciled assuming significantly smaller thermal conductivity and heat capacity at all temperatures from ambient to melting. The melting temperature is also smaller. It is suggested that these specific parameters are related to the photoinduced plasma. [S0031-9007(99)08806-7]

PACS numbers: 61.80.-x, 61.20.Ja, 64.70.Dv, 79.20.Ds

Pulsed laser melting of semiconductors is the basis of a wide range of surface processing techniques [1,2]: etching [3], cleaning [3], ablation, incorporation, and diffusion of specific foreign atoms into the substrate to obtain novel alloys or controlled doping depths [4–10]. Numerical simulations of heat diffusion and nonequilibrium melting [5,6] in the nanosecond regime have been developed to extract parameters describing superheating, undercooling, and impurity segregation. Simulations were compared to reflectivity, ellipsometry [7], transient conductance [8], and impurity depth profile [6] measurements. Recently, impurity desorption was also included [3]. A set of “standard” thermal and optical parameters of Si suitable to model satisfactorily laser annealing has been collected in Ref. [10] (Table I). Although such simulations have been useful to capture the essence of the ongoing processes, their accuracy can be questioned: The influence of impurities on the melting dynamics has been neglected, despite the fact that the experiments were carried out in air or in low vacuum. The presence of impurities at the surface may alter the optical and thermal properties of the substrate, especially in multipulse experiments where impurities may accumulate in the melted layer by diffusion from the surface. Obviously, understanding the adsorbate influence on the melting dynamics requires information concerning the melting of atomically clean surfaces. This is the purpose of the present work.

Up to now, ultrahigh vacuum (UHV) experiments have been concerned with the structure of the laser exposed surfaces measured by LEED [11] and STM [12] and not with the melting dynamics. The surface after recrystallization is atomically flat. Step ordering

is obtained more easily by laser than by heating [11], but various reconstructions can be obtained [12]. A site specific photodesorption of Si atoms [13] and of adsorbates [14] is observed below the melting threshold. In this work, we measure the transient reflectivity (TR) of Si(100) in UHV. We have pushed as far as we could the sensitivity of experiments (single pulse), the level of detail of simulations (reflectivity *below the melting threshold*) and the agreement between experiment and theory (fit of the TR—not just the melting duration or the melted depth—for a wide range of fluence and temperature). We compare the measured TR’s with numerical simulations of the heat flow, phase transition, and reflectivity, with the result that *the standard parameters are not appropriate for simulating the experiments*.

Experiments are carried out under a base pressure of  $2 \times 10^{-10}$  mbar on B-doped  $1.5 \Omega \text{ m}$  Si(100) surfaces. LEED and Auger are available for sample characterization. The Si sample is cleaned by standard methods. The intensity of a probe laser diode (cw, 675 nm, *s* polarized) is recorded with a time resolution of 2 ns after its reflection on the silicon sample. The reflected beam is passed through an interference filter and detected by a fast semiconductor detector, the linearity of which is carefully checked. Melting is induced by a pump XeCl laser at 308 nm. The angles of incidence are  $0^\circ$  and  $12^\circ$  for the pump and probe lasers, respectively. The pump pulse exhibits two peaks, the second peak being delayed by  $\approx 30$  ns (Fig. 1). The pump beam passes through a lens array homogenizer. The plane where the energy distribution is homogeneous is optically conjugated with the sample, the size of the uniformly irradiated area being

TABLE I. Standard (see text) and corrected thermal parameters used in the simulation. The corrected parameters are used only during the laser pulse, and only in a depth corresponding to the photoinduced plasma.

	Standard parameters [10]	Corrected parameters
Thermal conductivity ( $\text{W cm}^{-1} \text{K}^{-1}$ )	$T < 1200 \text{ K}: k_0 = 1552.98T^{-1.226}$ $T > 1200 \text{ K}: k_0 = 8.9956T^{-0.502}$	$k = 0.9k_0 - 0.12$
Specific heat ( $\text{J cm}^{-3} \text{K}^{-1}$ )	$C_0 = 1.611 \exp[2.375 \times 10^{-4} T]$	$C = C_0 - 0.18$
Melting temperature (K)	1683	1450

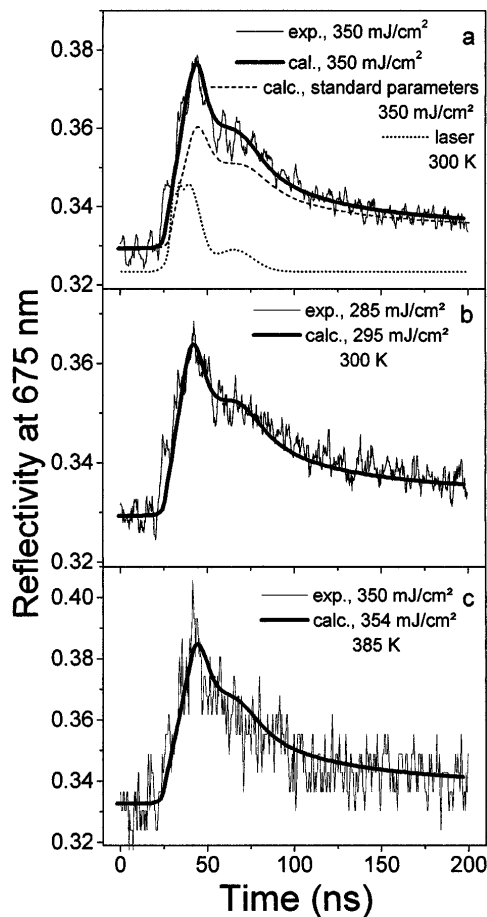


FIG. 1. Experimental and calculated transient reflectivity of Si under pulsed laser irradiation in UHV, for several initial surface temperature and laser fluences below the melting threshold. The modified thermal parameters (see text) are used for the calculated transients. For comparison, the transient reflectivity calculated using the “standard” parameters of Ref. [10] is also shown in (a). The typical temporal laser shape is shown in (a).

$\sim 2 \times 3 \text{ mm}^2$ . The size of the probe laser spot on the sample is  $0.1 \text{ mm}^2$ . Charges photoemitted by the excimer pulse are collected at 5 mm from the sample on a filament electrode (1 mm diameter, biased +90 V to the sample). At 308 nm only electrons of the conduction band can be photoemitted by absorption of one single photon. The photoelectron current thus reflects the electron population of the conduction band. All signals are recorded on a digital oscilloscope (500 MHz bandwidth) in one single laser shot.

Typical TR's below and above the melting threshold are displayed in Figs. 1 and 2, respectively (with a different scale of reflectivity). The TR shape is sensitive to the laser temporal profile. If Si is solid at the time of the second peak, a shoulder is visible in the TR because the second peak perturbs the cooling after the heating produced by the first peak. The TR height is smaller than 0.4 (the largest reflectivity of solid Si), and its width of  $\approx 20$  to 30 ns (ignoring the shoulder) is controlled essentially by heat flow and laser energy. Just above the melting threshold [Fig. 2(f)], the TR exhibits a narrow

peak with a width as small as 9 ns, which corresponds to melting. The height depends on the melted depth while the width is the melting duration. Both increase with laser fluence. The height saturates at the value of the reflectivity of liquid Si which is reached when the melted depth equals the absorption length of liquid Si at 675 nm. The width reaches  $\approx 100$  ns for  $660 \text{ mJ/cm}^2$  at 570 K. For large fluences, the simulations predict a hat shape, with two small maximas at the beginning and end of melting [Fig. 2(a)]. These correspond to optical interference effects by the thin liquid layer. After the adjustment of the thermal parameters described later, a feature remains unexplained, namely a decrease of the TR proportional to the laser power (best visible in Fig. 2(a)). This temporal signature suggests strongly that it is due to a plasma-induced change of the reflectivity of the liquid at 675 nm: the decay of the photoinduced plasma is at the sub-ns scale, while the thermal processes (cooling and recrystallization) have a time scale of several tens of ns.

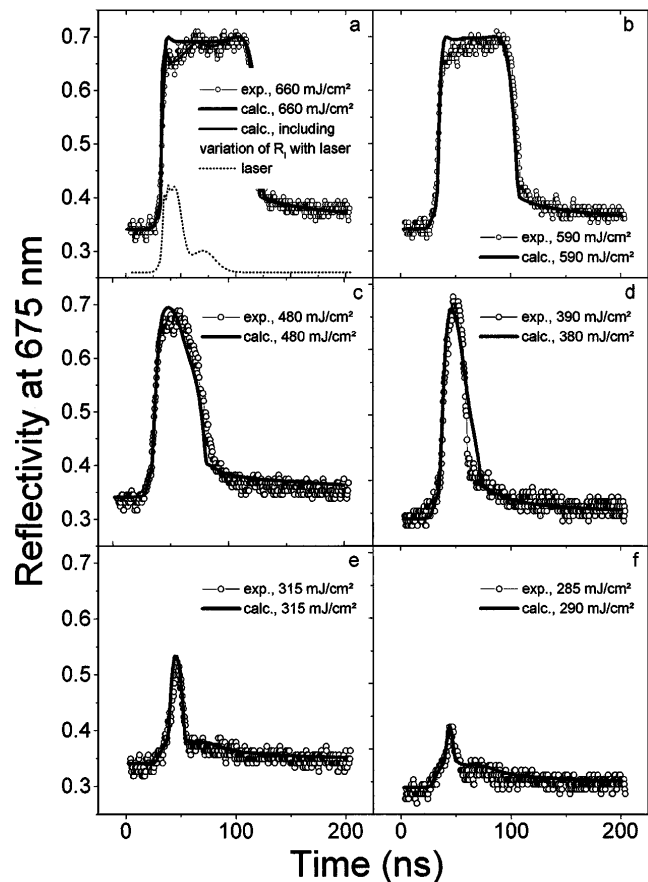


FIG. 2. Experimental and calculated transient reflectivity of Si under pulsed laser irradiation in UHV above the melting threshold. The initial surface temperature is 570 K. The modified thermal parameters (see text) are used for the calculated transients. In (a), a second simulation is also shown, where a linear variation with laser power of the reflectivity  $R_1$  of liquid Si is added (see text). The typical temporal laser shape is also shown in (a).

The large size of the pump laser beam with respect to the thermal diffusion length allows one to calculate the heat flow in one dimension (1D). The numerical resolution of the 1D heat flow equation provides the time and depth dependence of the substrate temperature which is used to calculate the TR's. For this purpose, not only the thickness of the liquid layer, but also the temperature gradient in the solid is taken into account [9], since the change of reflectivity due to heating alone is readily detectable by our system. Input data of our code are the optical parameters at the visible and UV wavelengths, the temporal shape of the laser pulse, and the thermal properties of the substrate. We simulated satisfactorily the melting duration corresponding to the data of de Unamuno *et al.* [10] and Jellison *et al.* [7], using the standard thermal parameters. Common features of these experiments are that they were carried out in air.

By contrast, our UHV data cannot be satisfactorily simulated using the same code and parameters. Figure 1(a) shows that the TR calculated with the standard parameters is smaller than the experimental one. This is a general result, that corresponds to a calculated melting threshold larger than the experimental one by  $\approx 250$  mJ/cm<sup>2</sup>. To understand the nature of the discrepancy, we use our numerical code in a fitting procedure, using the Si parameters as fitted parameters. Since the differences between experimental and calculated TR's exist already below the melting threshold, we first searched for a set of parameters appropriate to the solid. The parameters describing the liquid need not be considered to begin. We have to consider the possible variations of the UV and visible reflectivity, the absorption coefficient, the thermal conductivity, and the specific heat. We observe a slight *increase* of the UV reflectivity with laser fluence, in agreement with Ref. [10]. However a *decrease* of UV reflectivity is needed to reconcile experiment and theory. The absorption coefficient has a small effect on heating because the absorption depth ( $\approx 6$  nm) is much smaller than the heat diffusion length ( $\approx 1$   $\mu$ m at the time scale of the laser pulse). The hot carrier plasma photoinduced near the surface may affect the reflectivity, especially at 675 nm. As explained above, this effect is actually observed clearly on the liquid. As can be judged from Fig. 2, it is small and cannot account for the large difference between experiment and simulation with the standard parameters. The validity of the reflectivity variation with temperature may also be questioned, especially at high temperature [9], but the differences between experimental and calculated transients persist for low fluences, for which the temperature rise is smaller. We conclude that the thermal conductivity and the specific heat are the only parameters that can be varied.

In our fitting procedure, the analytic expressions of the thermal conductivity and specific heat are developed in a Taylor series with respect to temperature. The Taylor coefficients are used as fit parameters by comparison of the experimental and calculated TR's for three

sample temperatures (300, 385, and 575 K) and laser fluences from 250 to 750 mJ/cm<sup>2</sup>. The plausible causes of the discrepancy between experiment and theory are effects of the high temperature achieved that might not be properly taken into account by the equilibrium thermal parameters, and the presence of the photogenerated plasma. If only first or higher order terms of the Taylor series need to be modified with respect to the standard parameters, the cause of the modification is temperature dependent and cannot be ascribed to the photogenerated plasma. On the other hand, if the inclusion of the zero order term is necessary and quantitatively significant, the cause is likely to be the photogenerated plasma. *Attempts to fit the data using only high order terms (up to 6) of the Taylor series failed*, suggesting strongly that plasma effects are important. Therefore, *the thermal parameters were allowed to vary only during the laser pulse, and only in a depth corresponding to the diffusion of the photoinduced plasma*. Otherwise, our code keeps the standard values of Si. The diffusion depth of the photoinduced plasma is expected to depend in a complicated way on the electron energy and density distributions. Its order of magnitude was estimated using the model of Yoffa [15]. Since the melting dynamics is not very sensitive to it, a value of 50 nm was adopted in all cases. All the TR's below the melting threshold are satisfactorily fitted using the parameters listed in Table I.

Using the modified  $k$  and  $C$  to estimate the melting threshold shows an improvement of the agreement with experiment. A discrepancy of  $\approx 50$  mJ/cm<sup>2</sup> remains, which can be ascribed to a smaller melting temperature of 1450 K instead of 1683 K for pure crystalline silicon. The two modifications, of the thermal parameters and the melting temperature, limited to the solid and to a depth of 50 nm, are sufficient to allow a very satisfactory fit of all measured TR's as can be judged from Figs. 1 and 2.

The important result is that the correction that must be applied to the standard parameters concerns solid silicon over the entire temperature range from ambient to melting temperature, and that the correction applies only during laser irradiation. Other types of corrections failed. This shows that the problem with the standard parameters is related to the fact that they do not take into account a modification of the material that exists at all temperatures, and lasts only the time of the laser pulse, suggesting strongly that photoexcitation is responsible for the observed effects.

The corrected thermal conductivity and specific heat are smaller than the standard ones (Table I). Is this compatible with the interpretation that photoexcitation is responsible for the correction? Increasing slightly the density of conduction band electrons increases the conductivity. However, a large increase enhances strongly the recombination rate, therefore decreasing the electron mean free path, which in turn is expected to decrease the conductivity. A variation of the recombination rate with

electron density was observed experimentally over orders of magnitude after a fs excitation [16]. Can the observed decrease of the melting temperature be explained by photoexcitation? The properties of photoexcited Si were investigated theoretically by Silvestrelli *et al.* by molecular dynamics [17]. The liquid produced by a fs laser pulse differs from ordinary liquid Si by a reduction of covalent bonding and a larger coordination number. Melting results from the weakening of covalent bonds by electronic excitation, and from fast heating ( $\approx 100$  fs) of the ions by interaction with the photoexcited medium. Nonthermal laser melting of silicon by ultrashort pulses was confirmed experimentally [18–20]. Photoexcitation “helps” melting by allowing a second mechanism, more efficient in fs experiments than the electron-phonon interaction of time scale  $>1$  ps. It results that melting might be observed at a temperature lower than at equilibrium in ns experiments, providing that photoexcitation is large enough. An alternative point of view is that since neither solid nor liquid Si are in their normal states, the melting temperature has no reason to be equal to the equilibrium value, much like amorphous Si has not the same melting temperature (1350 K) as crystalline Si (1680 K).

The actual density of conduction band electrons is clearly a critical parameter, but it is difficult to evaluate. Silvestrelli *et al.* [17] have estimated a proportion of ionized atoms of 10% (or  $5 \times 10^{21} \text{ cm}^{-3}$ ) for a fs excitation. The proportion depends on the rates of excitation, diffusion, and recombination which do not scale linearly with the laser duration and energy. For a ns excitation, however, the proportion is undoubtedly smaller. At the laser fluence of the melting threshold, surface atoms are photoexcited every ns, a time scale comparable to that of recombination to the valence band, which largely exceeds 100 ps for a small density [16]. Experimentally, our photoemission measurements show that the total number of photoelectrons emitted per laser pulse varies smoothly with laser fluence across the melting threshold: There is no sharp increase related to melting, suggesting that the electron density in the conduction band in hot solid Si corresponds to that of a “metal” (liquid Si). The conduction electron density might be larger than  $10^{20} \text{ cm}^{-3}$ , well above a heavy doping, and this might modify sufficiently the thermal properties of Si.

In conclusion, we find that laser melting of Si surfaces in UHV can be simulated by a thermal model, but the equilibrium thermal parameters of Si are not adequate. They need to be corrected in a way that suggests that the photoinduced plasma modifies the Si thermal properties. In light of recent experiments and simulations of the literature at the fs time scale, it can also be speculated that melting occurs both through electron phonon interaction and through the mechanism responsible for melting in fs experiments [17]. The influence of adsorbates remains to be investigated. They may modify both the electronic

structure and the chemical composition of the melted layer. Although desorption occurs in the first ns [3], a significant fraction of impurities diffuse inside Si [21]. Their ultimate fate depends on segregation during recrystallization: At least a fraction of ML is present inside Si during melting, but this amount can be much larger in multipulse experiments.

We are indebted to D. Débarre and J. Boulmer for stimulating discussions and for sharing laser equipment. G. Lefèvre is acknowledged for his support during the experiments.

---

\*Corresponding author.

Electronic address: Bernard.Bourguignon@ppm.u-psud.fr

- [1] D. Bäuerle, *Chemical Processing with Lasers*, Springer Series in Materials Science (Springer, Berlin, 1986), Vol. 1.
- [2] I. W. Boyd, *Laser Processing of Thin Films and Microstructures*, Springer Series in Materials Science (Springer, Berlin, 1987), Vol. 3.
- [3] B. Dragnea, J. Boulmer, J.-P. Budin, D. Débarre, and B. Bourguignon, *Phys. Rev. B* **55**, 13 904 (1997).
- [4] A. Desmur, B. Bourguignon, J. Boulmer, J.-B. Ozenne, J.-P. Budin, D. Débarre, and A. Aliouchouche, *J. Appl. Phys.* **76**, 3081 (1994).
- [5] R. F. Wood, *Phys. Rev. B* **25**, 2786 (1982).
- [6] R. F. Wood and G. A. Geist, *Phys. Rev. B* **34**, 2606 (1986).
- [7] G. E. Jellison, Jr., D. H. Lowndes, D. N. Mashburn, and R. F. Wood, *Phys. Rev. B* **34**, 2407 (1986).
- [8] P. S. Peercy, M. O. Thompson, and J. Y. Tsao, *Appl. Phys. Lett.* **47**, 244 (1985).
- [9] G. E. Jellison, Jr. and F. A. Modine, *Phys. Rev. B* **27**, 7466 (1983); *J. Appl. Phys.* **76**, 3758 (1994).
- [10] S. De Unamuno and E. Fogarassy, *Appl. Surf. Sci.* **36**, 1 (1989).
- [11] D. M. Zehner, C. W. White, and G. W. Ownby, *Surf. Sci. Lett.* **92**, L67 (1980).
- [12] R. S. Becker, J. A. Golovchenko, G. S. Higashi, and B. S. Swartzentruber, *Phys. Rev. Lett.* **57**, 1010 (1986).
- [13] K. Ishikawa, J. Kanasaki, K. Tanimura, and Y. Nakai, *Solid State Commun.* **98**, 913 (1996).
- [14] K. Shudo, F. Komori, K. Hattori, and Y. Murata, *Surf. Sci.* **320**, 161 (1994).
- [15] E. J. Yoffa, *Phys. Rev. B* **21**, 2415 (1980).
- [16] M. C. Downer and C. V. Shank, *Phys. Rev. Lett.* **56**, 761 (1986).
- [17] P. L. Silvestrelli, A. Alvi, M. Parrinello, and D. Frenkel, *Phys. Rev. Lett.* **77**, 3149 (1996).
- [18] C. V. Shank, R. Yen, and C. Hirlimann, *Phys. Rev. Lett.* **51**, 900 (1983).
- [19] H. W. K. Tom, G. D. Aumiller, and C. H. Brito-Cruz, *Phys. Rev. Lett.* **60**, 1438 (1988).
- [20] P. Saeta, J. K. Wang, Y. Siegal, N. Bloembergen, and E. Mazur, *Phys. Rev. Lett.* **67**, 1023 (1991).
- [21] B. Bourguignon, M. Stoica, B. Dragnea, S. Carrez, J. Boulmer, J.-P. Budin, D. Débarre, and A. Aliouchouche, *Surf. Sci.* **338**, 94 (1995).